

Brain Tumor Identification using Improved YOLOv8

Rupesh Dulal¹ and Rabin Dulal²

¹Tribhuvan University, Nepal

²Charles Sturt University, Australia

Abstract—Identifying the extent of brain tumors is a significant challenge in brain cancer treatment. The main difficulty is in the approximate detection of tumor size. Magnetic resonance imaging (MRI) has become a critical diagnostic tool. However, manually detecting the boundaries of brain tumors from MRI scans is a labor-intensive task that requires extensive expertise. Deep learning and computer-aided detection techniques have led to notable advances in machine learning for this purpose. In this paper, we propose a modified You Only Look Once (YOLOv8) model to accurately detect the tumors within the MRI images. The proposed model replaced the Non-Maximum Suppression (NMS) algorithm with a Real-Time Detection Transformer (RT-DETR) in the detection head. NMS filters out redundant or overlapping bounding boxes in the detected tumors, but they are hand-designed and pre-set. RT-DETR removes hand-designed components. The second improvement was made by replacing the normal convolution block with ghost convolution. Ghost Convolution reduces computational and memory costs while maintaining high accuracy and enabling faster inference, making it ideal for resource-constrained environments and real-time applications. The third improvement was made by introducing a vision transformer block in the backbone of YOLOv8 to extract context-aware features. We used a publicly available dataset of brain tumors in the proposed model. The proposed model performed better than the original YOLOv8 model and also performed better than other object detectors (Faster R-CNN, Mask R-CNN, YOLO, YOLOv3, YOLOv4, YOLOv5, SSD, RetinaNet, EfficientDet, and DETR). The proposed model achieved 0.91 mAP (mean Average Precision)@0.5.

Index Terms—Brain tumor detection, Deep learning, Attention, Transformer, YOLOv8

I. INTRODUCTION

A brain tumor represents a dangerous disease resulting from abnormal and unwanted cell growth in the brain. A brain tumor is the cause of death for thousands of people around the world every year [1]. Medical experts use brain MRI imaging technology to detect portions of tumors. This is the best approach used in the medical diagnosis system. However, detecting tumors by analyzing the MRI images is labor-intensive, time-consuming, and can only be evaluated by the experts [2]. Therefore, an automatic and more straightforward solution is required to ease the process of brain tumor detection.

Brain tumors are of two types. One is malignant, and the other is non-malignant [3]. Malignant tumors can grow uncontrollably, invade surrounding tissues, and spread to other body parts. Malignant tumors are typically dangerous and require prompt treatment to prevent further spread and damage [4]. Non-malignant tumors, also known as benign tumors, are not

cancerous. They generally grow slowly and do not spread to other body parts. At the same time, benign tumors can still cause problems depending on their size and location [4]. A

primary brain tumor originates in the brain or spinal cord and starts to grow within these areas [5]. A type of brain tumor known as glioma is responsible for most primary brain and spinal cord cancers in adults. On the other hand, meningiomas represent the majority of noncancerous tumors. However, the situation is complicated because some meningiomas can act similarly to malignant tumors. At the same time, certain gliomas can be treated successfully and may stay in remission for many years or even be fully cured [5]. Malignant tumors are more damaging to humans and challenging to detect [6]. The primary purpose of this research is to help detect these two types of tumors from MRI photos using advanced technology.

In recent years, the advancement of artificial intelligence has shown impressive results in detecting and classifying brain tumors [2], [7]–[9]. Various conventional machine-learning techniques are used to detect and classify tumors [10]–[12]. However, traditional machine learning techniques cannot automatically extract the features from the raw data. They need various hand-designed feature extraction techniques that require computer experts' knowledge [13].

Convolutional Neural Network (CNN) is a deep learning model mostly used for processing data with a grid-like topology, like images. It is designed to automatically process the images as input and learn the features like textures, edges, and patterns. This process involves convolution layers and filters to extract or learn those local features. These patterns are combined and abstracted through deeper layers to recognize more complex structures, such as shapes or objects. CNNs are a compelling deep-learning method used for image recognition tasks [13]–[17]. CNNs are very popular and widely used deep learning methods for detecting, identifying, and classifying brain tumors [2], [8], [8], [9], [18]–[22].

Despite the powerful capabilities of CNNs in processing spatial data, they struggle with tasks that require handling long sequences and capturing long-range dependencies. This limitation arises because CNNs are not inherently designed to maintain context over very long sequences where understanding relationships across distant elements is crucial [23]. To address this gap, Transformer networks were developed. Transformers utilize self-attention mechanisms to capture dependencies across long sequences more effectively and enable

context-aware processing [23].

The Vision Transformer (ViT) is a transformer-based network for image recognition [24]. Unlike traditional CNNs, ViT treats an image as a sequence of patches, enabling it to effectively capture long-range dependencies and global context. By leveraging self-attention mechanisms, the Vision Transformer excels in tasks like image classification and object detection, offering a powerful alternative to conventional convolutional approaches [25], [26]. Thus, ViT has shown impressive applications in many brain tumor classifications because of its powerful and context-aware feature extraction capacity [27]–[30].

The deep learning-based detection method is more powerful and beneficial. However, deep learning-based methods are more computationally expensive, which provides a challenge for resource management and fast detection of tumors. This research aims to provide a better solution with a balance of accuracy and speed in detecting tumors. This research presents the following contributions:

- 1) This paper proposed a modified YOLOv8 [31] model for detecting brain tumors, incorporating several advanced components to enhance performance. First, we integrated a Vision Transformer [24] as a context-aware feature extraction block. ViT block helps to capture long-range dependencies within the input image features. Next, we utilized the RT-DETR [32] component to process these extracted features, employing an NMS-free detection head that enhances detection accuracy and efficiency. Additionally, we included Ghost Convolution [33] in our design, which provides a lighter convolution operation, reducing computational complexity without compromising the model’s effectiveness. Together, these modifications aim to improve the accuracy and efficiency of brain tumor detection.
- 2) We used a publicly available dataset and conducted extensive experiments in different object detection networks (Faster R-CNN [34], Mask R-CNN [35], YOLO [36], YOLOv3 [37], YOLOv4 [38], YOLOv5 [39], YOLOv8 [31], SSD [40], RetinaNet [41], EfficientDet [42], and DETR [43]) and compared the results with the proposed model. Our model outperformed the other object detection models.

II. BACKGROUND TERMS

This section provides a brief introduction and background knowledge to understand the different object detection models and terms used in this research.

Faster R-CNN uses a fully convolutional region proposal network (RPN). It uses an input image of any size and produces a set of regional proposals and objectiveness scores. Moreover, it uses multi-scale anchor boxes to classify and localize objects in different scales and aspect ratios. Anchor boxes are predefined bounding boxes that help the model handle multiple objects of different shapes and sizes more efficiently, improving detection performance. Using multi-scale anchor boxes and fully convolutional networks allows

Faster R-CNN to accurately and efficiently detect objects across different scales and aspect ratios within an image.

Mask R-CNN extends Faster R-CNN to deal with instance segmentation. The architecture of Mask R-CNN is composed of Feature Pyramid Networks (FPN) [35] with CNNs to extract hierarchical features (features extracted from the different levels of the deep networks having different sizes and resolutions). As we go deeper into the deep networks, the resolution of the feature maps decreases. FPN combines lower and higher-resolution feature maps in the network. In the first stage, RPN selects all feature maps generated by FPN and CNN (backbone) and generates region proposals. It also binds feature maps with locations in the original image using anchor boxes. The second stage uses another neural network to classify and localize the image.

SSD is a popular object detection model that performs object localization and classification in a single shot. It uses a single neural network to predict multiple bounding boxes and their corresponding class probabilities for objects of various sizes within an image. SSD achieves efficiency by applying convolutional filters to feature maps at different scales to detect objects at multiple resolutions simultaneously. This method allows SSD to be fast and suitable for real-time object detection tasks.

RetinaNet is another object detection model designed to address the problem of class imbalance in object detection datasets, where the number of background (non-object) samples far exceeds the number of object samples. RetinaNet introduces a novel focal loss function [41] that down-weights the loss assigned to well-classified examples and focuses more on complex, misclassified examples during training. This focal loss helps RetinaNet perform better, especially when detecting objects at various scales and dealing with imbalanced datasets.

EfficientDet is a family of object detection models that aims to balance accuracy and efficiency by leveraging the principles of model scaling and compound scaling. EfficientDet builds upon the EfficientNet [44] architecture, which optimizes model depth, width, and resolution based on a compound coefficient. EfficientDet uses EfficientNet as a backbone network and Bidirectional Feature Pyramid Network (BiFPN) [42] in the head network to enhance multi-scale feature fusion and better detection accuracy. BiFPN is an advanced FPN designed to improve the efficiency and effectiveness of multi-scale feature fusion in object detection models. Its bidirectional and weighted fusion approach makes it a powerful component for achieving high performance in object detection [42]. EfficientDet achieves state-of-the-art performance with significantly fewer parameters than other models. This makes EfficientDet well-suited for resource-constrained environments or applications requiring real-time inference.

YOLO approaches the object detection problem as a single regression problem, where the network directly predicts bounding boxes and class probabilities from a full image in one evaluation using CNN. This differs from traditional methods involving generating region proposals and performing classification separately. The algorithm divides the input image

into a grid of cells, and each cell is responsible for predicting multiple bounding boxes and their associated confidence scores. YOLO employs Intersection over Union (IoU) to measure the accuracy of predicted bounding boxes against ground truth and uses non-maximum suppression to select the most accurate bounding box if multiple are generated for the same object. Each bounding box prediction includes parameters for the box's center (x, y) relative to the grid cell, its width (w) and height (h) relative to the entire image, and a confidence score representing the IoU with the ground truth object. This approach allows YOLO to detect objects in real time with a single pass through the network. **YOLOv3** is an improvement over YOLO, designed to be faster and more accurate. It introduces several key enhancements, including FPN, to extract features at different scales, enabling the detection of objects of varying sizes. It uses a deeper type of CNN called Darknet-53 [37] backbone network for better feature extraction, enhancing the model's ability to capture complex image patterns. Moreover, it predicts bounding boxes and class probabilities simultaneously at three different scales to detect objects of various sizes more effectively (in the head network of YOLOv3). **YOLOv4** further improves its backbone by introducing Cross Stage Partial (CSP) [45] on Darknet53. CSP connection is a design strategy used in deep networks to improve learning efficiency and reduce computational complexity. Moreover, it incorporates various optimization techniques, such as Bag of Freebies (BoF), and architectural modifications, such as Bag of Specials (BoS), to enhance performance. **YOLOv5** utilizes advanced training strategies such as mosaic data augmentation and self-ensembling for improved performance and enhanced post-processing techniques for more accurate bounding box predictions. Mosaic data augmentation is a powerful technique that enhances training datasets by combining four same or different images into one, thereby increasing variation and improving the model's ability to generalize and detect objects under various conditions [46]. **YOLOv8** introduces several enhancements over its predecessors, including more efficient architecture and improved training strategies, which lead to better performance in real-time object detection tasks. It maintains the core principle of YOLO by predicting bounding boxes and class probabilities directly from images in a single pass, making it highly effective for applications requiring fast and accurate detection. **DETR** has demonstrated impressive performance on object detection benchmarks, showcasing the potential of transformer-based architectures for complex computer vision tasks. By leveraging the transformer's ability to model global context and dependencies, DETR offers a novel approach to object detection that eliminates the need for many design choices and hyperparameters associated with traditional anchor-based methods. DETR is free of hand-designed components like anchor boxes and non-maximum suppression (NMS), and directly predicts the object class and bounding box. It uses a CNN backbone (pre-trained ResNet50) and transformer architecture in the head to detect the objects.

RT-DETR is a state-of-the-art object detection model that delivers real-time performance without compromising accu-

racy. Inspired by the DETR framework, which eliminates the need for Non-Maximum Suppression (NMS), RT-DETR incorporates a convolutional backbone and an optimized hybrid encoder to achieve rapid processing speeds. The model effectively handles multiscale features by separating intra-scale interactions from cross-scale fusion. Additionally, RT-DETR is highly versatile, allowing for flexible adjustments in inference speed by modifying decoder layers without requiring retraining. This is an improved version of DETR, which minimizes the significant computational complexity in DETR.

GhostConv A ghost convolution (GhostConv) is a component used in the architecture of GhostNet [33], which is a type of convolutional neural network (CNN) designed to be more efficient in terms of computational cost and model size. Feature maps obtained from Conv often contain a significant amount of redundancy, with many feature maps being similar. It is inefficient to rely solely on expensive convolution operations to generate these redundant feature maps. The GhostConv addresses this inefficiency by using cheaper linear operations (Ghost Bottlenecks) to extract feature maps after the initial convolution. This approach allows the GhostConv block to achieve more functional outcomes than traditional convolution operations but with fewer parameters and lower computational costs. By reducing redundancy and focusing computational resources more efficiently, the Ghost module enhances the network's overall efficiency without compromising performance.

Transformer Encoder (TE) TE are the vision transformer-based components without the layer normalization. A sketch of TE is shown in Figure 1. TE uses embedded patches as input and processes using its major components, multi-head attention and multilayer perceptron (MLP).

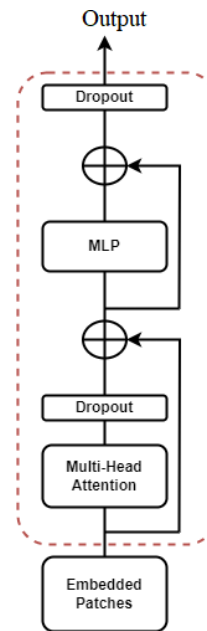


Fig. 1. The architecture of the transformer encoder, which contains multi-head attention and MLP layers.

TE first divides an image into non-overlapping patches of the same sizes. Each patch of the image is like a single RGB channel image, which is then converted into a 1-dimensional vector called patch embedding. To make the sequence of the patches meaningful and in a fixed order, positional encoding is applied to each vector resulting from each patch. The patches with positional encoding are called embedded patches. An alternate sine and cosine functions calculate positional encoding as:

$$PE_{(pos,2i)} = \sin(pos/10000^{2i/d_{model}}) \quad (1)$$

$$PE_{(pos,2i+1)} = \cos(pos/10000^{2i/d_{model}}) \quad (2)$$

where:

- d_{model} : The dimension of the embeddings in the TE. For example, if the embeddings are 512-dimensional vectors, then $d_{model} = 512$.
- PE: Positional encoding value for a given position pos and dimension index $2i$ or $2i + 1$.
- pos : The token's position in the sequence (e.g., the 1st, 2nd, 3rd token, etc.).
- i : The index of the dimension of the positional encoding vector, running from 0 to $\frac{d_{model}}{2} - 1$.

The multi-head attention block has three unique parameters: the query (Q), key (K), and value (V). In simple words, the query is the information to be processed, the key is the relevance of the information, and the value is the summary of the query and its relevance to the different individual components within the input sequence. The W^Q , W^K , and W^V are learnable weight matrices corresponding to query, key, and value i . These parameters are initially assigned with random values and then learned during the backpropagation. For an input sequence vector X ,

$$Q, K, V = XW^Q, XW^K, XW^V$$

Q , K , and V are the matrix multiplication of the input sequence vector and the respective learnable parameters. The following equations obtain the outputs of the attention weights.

$$\text{Attention}(Q, K, V) = \text{softmax} \left(\frac{QK^T}{d_k} \right) V \quad (3)$$

The attention scores of Q , K , and V are scaled by $\frac{1}{d_k}$ before applying the softmax function where d_k is the dimension of the key. This is the attention of one head. The final output of the multi-head attention (MHA) block is obtained by the concatenation of the attention scores of each head through a linear transformation as obtained by the following equation:

$$\text{MHA}(Q, K, V) = \text{Concat}(\text{head}_1, \dots, \text{head}_h) \cdot W_o \quad (4)$$

where W_o is a weight matrix and each head i is computed as:

$$\text{head}_i = \text{Attention}(Q_i, K_i, V_i) \quad (5)$$

MLP is two fully connected networks in a feed-forward fashion. Residual connections are used between each layer of the TE as shown in Figure 1.

III. RELATED WORKS

The primary objective of this research is the identification of brain tumors. This section includes the latest methods applied to brain tumor identification approaches. The earlier machine learning and hand-crafted methods are not included in this literature. Notable deep-learning solutions for accurately identifying brain tumors are included in this section.

There are numerous research based on CNNs to classify the types of tumors accurately [22], [47]–[54]. However, the classification of the tumors does not provide the exact location of the tumors in the MRI. The classification only provides information on whether the specific MRI contains tumors. The main problem is to approximate the location and types of the tumors.

Many researchers focus on the detection and segmentation of tumors [55]–[64]. However, they failed to provide a comparative study of various object detection methods that match the accuracy and speed in detecting brain tumors.

This highlights the opportunity to develop a method for accurately identifying tumors, including pinpointing their exact location and determining the specific type of tumor. This research compares the 11 most popular object detection methods applied for identifying brain tumors. In addition, a novel improved YOLOv8 is proposed for the first time in brain tumor identification. The proposed method outperformed the existing 11 object detection methods in accuracy. This research provides the best solution for medical doctors or experts to locate the area and the type of tumors in MRI images, showcasing excellence.

IV. METHODOLOGY

A simple pipeline of the proposed methodology is shown in Fig. 2. The MRI brain images are first pre-processed to meet the requirements of the improved YOLOv8 model. These pre-processed images are then used to train and validate the proposed YOLOv8 model. Ultimately, the model is employed to identify tumors in the images. This section will briefly discuss the proposed methodology for effectively identifying brain tumors.

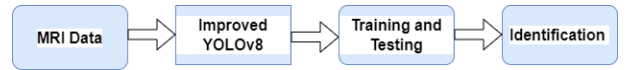


Fig. 2. A high-level sketch of the proposed brain tumor identification methodology.

A. Datasets Description

We utilized a publicly available dataset from Kaggle [65], which includes MRI images of brain tumors, specifically glioma and meningioma, and images without tumors. The dataset is divided into 878 images for training and 223 for validation, providing diverse examples to train and evaluate our model effectively.

B. Data Pre-processing

The dataset is annotated with bounding boxes using Roboflow [66] to adhere to the YOLOv8 format. We applied data augmentation techniques to enhance the model's robustness and increase the number of training samples. These techniques include rotations of +15 and -15 degrees and horizontal and vertical flips. These augmentations help the model generalize better by exposing it to various image orientations and perspectives.

C. YOLOv8

To fully understand the improved YOLOv8, we first describe the architecture of YOLOv8. YOLOv8 is the combination of various modules and techniques used in deep learning. The architecture of YOLOv8 [31] is sketched in Figure 3. YOLOv8 is a one-stage object detection model that consists of backbone, neck, and head modules. Backbone is used to extract the features from the images in different scales. The neck combines the different features and passes to the head. The head is used to detect (classify and localize) the object. A detailed explanation of each module is presented as follows:

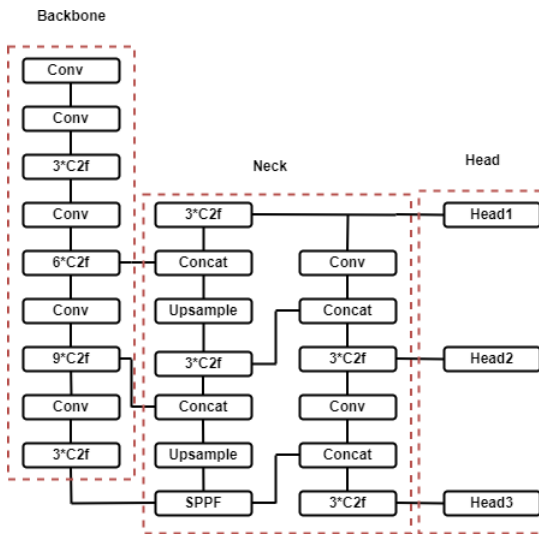


Fig. 3. The architecture of the YOLOv8. It consists of a backbone, neck, and head modules.

1) *Backbone*: The backbone consists of several blocks of convolution layers (Conv), C2f module, and Spatial Pyramid Pooling-Fast (SPPF). Conv is a convolution block consisting of a 2D convolution applied to the input image, batch normalization [67], and Sigmoid-weighted Linear Unit (SiLU) [68] activation function. SiLU is an improvement over Rectified Linear Unit (ReLU) [69]. SiLU does not have fixed upper or lower bounds, unlike the Sigmoid function (which is bounded between 0 and 1). This allows SiLU to avoid saturation issues where gradients can vanish, a common problem with Sigmoid in deep networks.

The C2f module in YOLOv8 is a streamlined and faster variant of the CSP (Cross Stage Partial) [45] Bottleneck with two convolutions (C2). Designed to enhance the execution speed

without compromising performance. C2f introduces modifications that optimize the original C2 module. The C2f module consists of an initialization phase where the input channels are mapped to fewer hidden channels using a convolutional layer. This initial layer splits the input into two parts, then processed in parallel. The module includes a series of Bottleneck blocks, each processing the output from the preceding block. The processed outputs are then concatenated along with the initial split and passed through another convolutional layer, which combines and refines the features. An alternative forward method further optimizes the processing, offering additional speed improvements. Overall, the C2f module is an efficient building block that maintains the architectural integrity of the original CSP Bottleneck while providing faster processing for the YOLOv8 model. The different numbers (like 3 numbers of C2f represented by 3*C2f in Figure 3) of the C2f blocks are stacked by adopting residual connection, and feature maps extracted by three levels of C2f are forwarded to the neck module. These three levels (also called feature layers) of C2f have feature maps of different dimensions. The first layer from the top extracts less semantic information. As the depth of the backbone increases, more semantic information is extracted, and the size of feature maps keeps decreasing. Thus, the lowest feature layer extracts high semantic information, but the feature map size is the smallest.

2) *Neck*: The outputs of the C2f blocks are passed to the SPPF block. It is an improvement of Spatial Pyramid Pooling (SPP) [70] by replacing large-sized kernels with small-sized kernels for faster operations. SPPF is a powerful technique that provides a multi-scale representation of input feature maps, capturing features at various levels of abstraction (dimensions). This capability is particularly useful for object detection, where detecting objects of different sizes is essential for achieving high accuracy and robustness.

The neck of YOLOv8 is inspired by the working mechanism of the Feature Pyramid Network (FPN) [71] and Path Aggregation Network (PANet) [72]. FPN is a pyramid-style structure mainly used to combine features of different scales. The backbone extracts features at three levels of abstraction with varying sizes. These different-sized feature maps are upsampled to match the size of feature maps of different feature levels and concatenated. PANet enhances the FPN architecture by incorporating a bottom-up path augmentation. This additional pathway allows position information from lower levels of the network to be effectively transmitted to higher levels. As a result, the positioning capabilities of the network are improved across multiple scales. This bottom-up approach complements the original top-down pathway of the backbone, ensuring that detailed spatial information from early layers is preserved and utilized in deeper layers, leading to better performance in tasks requiring multi-scale feature representation.

3) *Head*: In YOLOv8, three heads are designed to detect objects of various sizes. Specifically, these heads target objects at three different scales. They are for large, medium, and small objects. Figure 3 shows three heads: head1 is designed to

detect large objects, head2 for medium objects, and head3 for small objects. The heads create grids on these feature maps based on their respective dimensions. Each grid cell is responsible for predicting bounding boxes at its location. Three groups of anchors with different aspect ratios are predefined for each grid cell on each feature map. These anchors serve as reference bounding boxes to generate candidate bounding boxes for object detection. After generating the candidate bounding boxes, Non-Maximum Suppression (NMS) [73] is applied. NMS is a post-processing step that removes overlapping bounding boxes by keeping only the ones with the highest confidence scores. This step ensures that the final output consists of bounding boxes with their locations, sizes, and the associated confidence scores of the detected objects, minimizing redundancy and improving detection accuracy. The head provides the bounding box of the detected objects, class name, and the confidence score.

D. Improved YOLOv8

The proposed Improved YOLOv8 is motivated by the success of Vision Transformer (ViT) [24] in computer vision tasks. ViT is a transformer [23]-based architecture adapted for computer vision tasks which shows state-of-the-art performance in image recognition [24]. It replaces the convolutional layers in traditional computer vision models with self-attention mechanisms. This allows the model to attend to different regions of an image flexibly and adaptively, extracting rich features.

The sketch of the proposed architecture is shown in Figure 4. The proposed model modifies the YOLOv8 model in the backbone, neck, and head modules by replacing the last C2f block of the backbone with the Vision Transformer encoder (TE) block and the Conv block with the GhostConv block. The YOLOv8 head has NMS as the post-processing step. But they are hand-designed and fixed components. They cannot be changed according to the size of the objects. This means that the same IoU threshold and suppression criteria are applied uniformly across all detected objects, regardless of their size or context. As a result, the fixed nature of NMS might not be optimal for all situations, particularly when dealing with objects of varying sizes or in cases where the standard IoU threshold doesn't suit the specific detection scenario [43]. To address the limitations of the NMS, a dynamic head is used in this improved YOLOv8. The improved YOLOv8 has an RT-DETR head, providing more accurate identification accuracy without hand-designed NMS components.

E. Implementation

The experiment was conducted and implemented using the Pytorch library. For all experiments conducted for this research, the same hyperparameters are used to implement all selected models and are given in Table I.

F. Evaluation Criteria

The performance of the selected models is evaluated using standard metrics, mean Average Precision (mAP), and inference time. mAP and inference time are essential evaluation

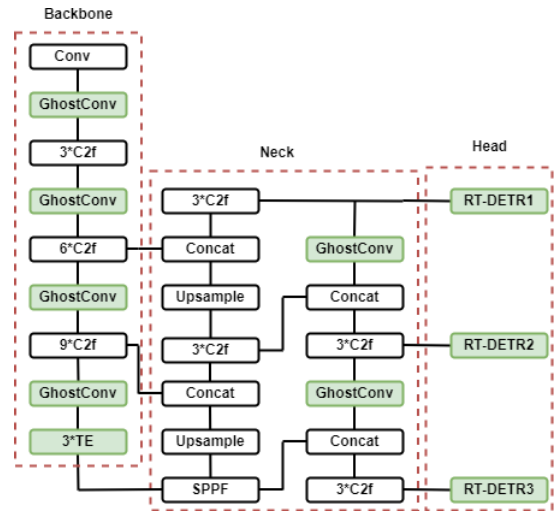


Fig. 4. The proposed architecture of Improved-YOLOv8. It has modifications on the backbone, neck, and head modules. The green boxes represent the improved part.

TABLE I
HYPERPARAMETERS FOR THE CONDUCTED EXPERIMENTS IN THIS RESEARCH.

Epochs	200
Batch size	16
Learning rate	0.01
Momentum for SGD	0.95
Weight decay for regularization	0.0005
Graphical Processing Unit (GPU)	Tesla T4, 15 GB

metrics for object detection models, offering insights into the models' accuracy and speed. mAP is a common criterion for measuring object detection performance. The mAP is calculated by calculating the average precision (AP) for each class and then the mean value of AP over all classes as below:

$$Precision(P) = \frac{TP}{TP + FP}$$

$$Recall(R) = \frac{TP}{TP + FN}$$

$$AP = \int_0^1 P(R) dR$$

$$mAP = \frac{1}{c} \sum_{i=1}^c AP_i$$

where c is the classes number.

where TP , FP , and FN stand for true positive, false positive, and false negative, respectively.

TP: A true positive is a case when the model correctly identifies and localizes an object within an image. This means the predicted bounding box sufficiently overlaps with the ground truth bounding box of the object. Ground truth refers to the actual, real-world data manually labeled or annotated. It serves as a reference or benchmark against which the performance of models is evaluated.

FP: A false positive is a case when the model detects an object that is not in the image or mislocalizes the object by providing a bounding box that significantly deviates from the actual object location or ground truth.

FN: A false negative in object detection refers to a situation where the model cannot detect an object in an image. This happens when the model either misses the object completely or provides a bounding box that does not adequately capture the object.

Intersection over Union (IoU) is a metric frequently employed in computer vision tasks. Given two sets of pixels, AA representing the detected object and BB representing the true object, the IoU is calculated as:

$$IoU(A, B) = \frac{A \cap B}{A \cup B}$$

The metric mAP@0.5 refers to the mean Average Precision (mAP) computed when the IoU exceeds 50%. This score comprehensively assesses an object detection model’s accuracy across various classes. mAP@0.5 is used as a threshold in the evaluation metric because it is a standard metric and threshold used by PASACL VOC object detection challenge [74].

G. Comparison With Existing Object Detection Models

The comparative analysis of the performance of the selected models and our proposed model is presented in Table II. Table II presents a comparative analysis of various object

TABLE II
COMPARATIVE RESULT OF THE BRAIN TUMOR IDENTIFICATION PERFORMANCE

Models	mAP@0.5
Faster R-CNN	0.68
Mask R-CNN	0.72
SSD	0.61
RetinaNet	0.73
EfficientDet	0.82
DETR	0.79
YOLO	0.65
YOLOv3	0.85
YOLOv4	0.84
YOLOv5	0.88
YOLOv8	0.87
Improved YOLOv8 (Our)	0.91

detection models for brain tumor identification, showcasing their performance based on the mean Average Precision (mAP) at a 0.5 IoU threshold. Traditional models like Faster R-CNN and SSD show moderate performance with mAP scores of 0.68 and 0.61, respectively. More advanced models such as RetinaNet, EfficientDet, and DETR demonstrate improved accuracy, with mAP scores ranging from 0.73 to 0.82. The YOLO series of models, particularly YOLOv3, YOLOv4, and YOLOv5, achieve higher accuracy, with mAP scores of 0.85, 0.84, and 0.88, respectively. Notably, the improved YOLOv8 model proposed in our work outperforms all other models, achieving the highest mAP of 0.91, highlighting its superior effectiveness in accurately identifying brain tumors.

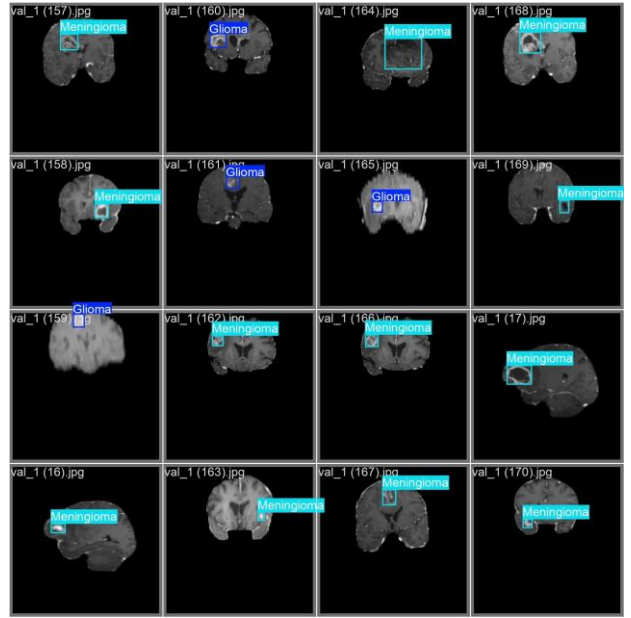


Fig. 5. A sample of the identified tumors. The bounding box provides the location of the tumors with the type of tumors.

A sample of identified tumors obtained from the proposed model is shown in Fig. 5.

The improved YOLOv8 proposed in this research shows impressive performance for the following reasons.

- Replacing the last C2f block with a TE block introduces better global context understanding. Transformers excel at capturing long-range dependencies and relationships between different parts of an image, which can enhance feature representation, especially in complex scenes where contextual information is crucial.
- Ghost Convolution is designed to reduce the number of parameters and computational cost while maintaining or even improving the representative capacity of the model. By generating "ghost" feature maps that approximate the full convolutional operation, this approach makes the model more efficient and lightweight, leading to faster inference times and potentially better generalization.
- Replacing the normal YOLOv8 head with RT-DETR improves the detection process by leveraging the strengths of transformer-based detection heads. RT-DETR is designed for real-time object detection, offering efficient handling of object relations and better performance, particularly in complex scenes. It also typically has more adaptive post-processing, which could address some limitations of fixed NMS providing dynamic tumor identification.
- The combination of ViT and Ghost Convolution improves feature extraction at multiple levels, ensuring that the model captures local and global features more effectively. This results in more robust representations, leading to better detection accuracy.

V. CONCLUSION

In conclusion, our research presents a significant advancement in the automated detection of brain tumors by introducing an enhanced YOLOv8 model. Through strategic modifications, including the integration of a Vision Transformer block, Ghost Convolution, and RT-DETR, our proposed model achieves a final accuracy of 0.91 mAP@0.5. This performance surpasses that of 11 popular object detection methods, as validated on a publicly available dataset. The improved accuracy and efficiency of our model provide a reliable tool for medical professionals, aiding in the accurate and timely detection of brain tumors using MRI images. This contribution has the potential to enhance diagnostic processes and patient outcomes in clinical settings.

REFERENCES

- [1] D. Bechet, S. R. Mordon, F. Guillemin, and M. A. Barberi-Heyob, "Photodynamic therapy of malignant brain tumours: A complementary approach to conventional therapies," *Cancer treatment reviews*, vol. 40, no. 2, pp. 229–241, 2014.
- [2] K. R. Pedada, B. Rao, K. K. Patro, J. P. Allam, M. M. Jamjoom, and N. A. Samee, "A novel approach for brain tumour detection using deep learning based technique," *Biomedical Signal Processing and Control*, vol. 82, p. 104549, 2023.
- [3] E. T. Fossel, J. M. Carr, and J. McDonagh, "Detection of malignant tumors," *New England Journal of Medicine*, vol. 315, no. 22, pp. 1369–1376, 1986.
- [4] A. F. Tamimi, I. Tamimi, M. Abdelaziz, Q. Saleh, F. Obeidat, M. Al-Husseini, W. Haddadin, and F. Tamimi, "Epidemiology of malignant and non-malignant primary brain tumors in Jordan," *Neuroepidemiology*, vol. 45, no. 2, pp. 100–108, 2015.
- [5] T. U. of Kansas Cancer Center, "Brain tumors," 2024, accessed: 2024-08-25. [Online]. Available: <https://www.kucancercenter.org/cancer/cancer-types/brain-cancer/>
- [6] E. F. Badran, E. G. Mahmoud, and N. Hamdy, "An algorithm for detecting brain tumors in MRI images," in *The 2010 International Conference on Computer Engineering & Systems*. IEEE, 2010, pp. 368–373.
- [7] D. A. Dahab, S. S. Ghoniemy, G. M. Selim *et al.*, "Automated brain tumor detection and identification using image processing and probabilistic neural network techniques," *International journal of image processing and visual communication*, vol. 1, no. 2, pp. 1–8, 2012.
- [8] P. T. Selvy, V. Dharani, and A. Indhuja, "Brain tumour detection using deep learning techniques," *Int. J. Sci. Res. Comput. Sci. Eng. Inf. Technol.*, vol. 169, p. 175, 2019.
- [9] S. Maharjan, A. Alsadoon, P. Prasad, T. Al-Dalain, and O. H. Alsadoon, "A novel enhanced softmax loss function for brain tumour detection using deep learning," *Journal of neuroscience methods*, vol. 330, p. 108520, 2020.
- [10] S. Giraddi and S. Vaishnavi, "Detection of brain tumor using image classification," in *2017 International Conference on Current Trends in Computer, Electrical, Electronics and Communication (CTCEEC)*. IEEE, 2017, pp. 640–644.
- [11] M. Gurbina, M. Lascu, and D. Lascu, "Tumor detection and classification of MRI brain image using different wavelet transforms and support vector machines," in *2019 42nd International Conference on Telecommunications and Signal Processing (TSP)*. IEEE, 2019, pp. 505–508.
- [12] A. Halder, C. Giri, and A. Halder, "Brain tumor detection using segmentation based object labeling algorithm," in *International Conference on Electronics, Communication and Instrumentation (ICECI)*. IEEE, 2014, pp. 1–4.
- [13] Y. LeCun, Y. Bengio, and G. Hinton, "Deep learning," *nature*, vol. 521, no. 7553, pp. 436–444, 2015.
- [14] Z. Li, F. Liu, W. Yang, S. Peng, and J. Zhou, "A survey of convolutional neural networks: analysis, applications, and prospects," *IEEE Transactions on Neural Networks and Learning Systems*, 2021.
- [15] K. O'shea and R. Nash, "An introduction to convolutional neural networks," *arXiv preprint arXiv:1511.08458*, 2015.
- [16] J. Gu, Z. Wang, J. Kuen, L. Ma, A. Shahroudy, B. Shuai, T. Liu, X. Wang, G. Wang, J. Cai *et al.*, "Recent advances in convolutional neural networks," *Pattern recognition*, vol. 77, pp. 354–377, 2018.
- [17] R. Yamashita, M. Nishio, R. K. G. Do, and K. Togashi, "Convolutional neural networks: an overview and application in radiology," *Insights into imaging*, vol. 9, pp. 611–629, 2018.
- [18] A. Chattopadhyay and M. Maitra, "MRI-based brain tumour image detection using CNN based deep learning method," *Neuroscience informatics*, vol. 2, no. 4, p. 100060, 2022.
- [19] K. Bathe, V. Rana, S. Singh, and V. Singh, "Brain tumor detection using deep learning techniques," in *Proceedings of the 4th International Conference on Advances in Science & Technology (ICAST2021)*, 2021.
- [20] S. Bagyaraj, R. Tamilselvi, P. B. Mohamed Gani, and D. Sabarinathan, "Brain tumour cell segmentation and detection using deep learning networks," *IET Image Processing*, vol. 15, no. 10, pp. 2363–2371, 2021.
- [21] S. Kumar, N. Kumar, I. K. Rishabh, V. Keshari *et al.*, "Automated brain tumour detection using deep learning via convolution neural networks (CNN)," *Int. J. Cur. Res. Rev.*, vol. 13, no. 02, p. 148, 2021.
- [22] V. K. Waghmare and M. H. Kolekar, "Brain tumor classification using deep learning," *Internet of things for healthcare technologies*, pp. 155–175, 2021.
- [23] A. Vaswani, N. Shazeer, N. Parmar, J. Uszkoreit, L. Jones, A. N. Gomez, L. Kaiser, and I. Polosukhin, "Attention is all you need," *Advances in neural information processing systems*, vol. 30, 2017.
- [24] A. Dosovitskiy, L. Beyer, A. Kolesnikov, D. Weissenborn, X. Zhai, T. Unterthiner, M. Dehghani, M. Minderer, G. Heigold, S. Gelly *et al.*, "An image is worth 16x16 words: Transformers for image recognition at scale," *arXiv preprint arXiv:2010.11929*, 2020.
- [25] S. Khan, M. Naseer, M. Hayat, S. W. Zamir, F. S. Khan, and M. Shah, "Transformers in vision: A survey," *ACM computing surveys (CSUR)*, vol. 54, no. 10s, pp. 1–41, 2022.
- [26] N. Park and S. Kim, "How do vision transformers work?" *arXiv preprint arXiv:2202.06709*, 2022.
- [27] S. Tummala, S. Kadry, S. A. C. Bukhari, and H. T. Rauf, "Classification of brain tumor from magnetic resonance imaging using vision transformers ensembling," *Current Oncology*, vol. 29, no. 10, pp. 7498–7511, 2022.
- [28] E. S. ahin, D. O. zdemir, and H. Temurtas, "Multi-objective optimization of vit architecture for efficient brain tumor classification," *Biomedical Signal Processing and Control*, vol. 91, p. 105938, 2024.
- [29] S. Hong, J. Wu, L. Zhu, and W. Chen, "Brain tumor classification in vit-b/16 based on relative position encoding and residual MLP," *Plos one*, vol. 19, no. 7, p. e0298102, 2024.
- [30] M. A. L. Khaniki, A. Golkari, and M. Manthouri, "Brain tumor classification using vision transformer with selective cross-attention mechanism and feature calibration," *arXiv preprint arXiv:2406.17670*, 2024.
- [31] Ultralytics, "The state-of-the-art yolo model," <https://ultralytics.com/yolov8>, (accessed: 15.01.2023).
- [32] Y. Zhao, W. Lv, S. Xu, J. Wei, G. Wang, Q. Dang, Y. Liu, and J. Chen, "Detrs beat yolos on real-time object detection," in *Proceedings of the IEEE/CVF Conference on Computer Vision and Pattern Recognition*, 2024, pp. 16 965–16 974.
- [33] K. Han, Y. Wang, Q. Tian, J. Guo, C. Xu, and C. Xu, "Ghostnet: More features from cheap operations," in *Proceedings of the IEEE/CVF conference on computer vision and pattern recognition*, 2020, pp. 1580–1589.
- [34] S. Ren, K. He, R. Girshick, and J. Sun, "Faster r-cnn: Towards real-time object detection with region proposal networks," *Advances in Neural Information Processing Systems (NeurIPS)*, vol. 28, pp. 91–99, 2015.
- [35] K. He, G. Gkioxari, P. Dollár, and R. Girshick, "Mask r-cnn," in *Proceedings of the IEEE/CVF International Conference on Computer Vision (ICCV)*, 2017, pp. 2961–2969.
- [36] J. Redmon and A. Farhadi, "YOLO9000: better, faster, stronger," in *Proceedings of the IEEE/CVF Conference on Computer Vision and Pattern Recognition (CVPR)*, 2017, pp. 7263–7271.
- [37] —, "Yolov3: An incremental improvement," *arXiv preprint arXiv:1804.02767*, 2018.
- [38] A. Bochkovskiy, C.-Y. Wang, and H.-Y. M. Liao, "YOLOv4: Optimal speed and accuracy of object detection," *arXiv preprint arXiv:2004.10934*, 2020.
- [39] "YOLOv5," <https://github.com/ultralytics/yolov5>, (accessed 12 Jan 2023).
- [40] Z. Li and F. Zhou, "FSSD: feature fusion single shot multibox detector," *arXiv preprint arXiv:1712.00960*, 2017.

- [41] T.-Y. Lin, P. Goyal, R. Girshick, K. He, and P. Dolla' r, "Focal loss for dense object detection," in *Proceedings of the IEEE/CVF International Conference on Computer Vision (ICCV)*, 2017, pp. 2980–2988.
- [42] M. Tan, R. Pang, and Q. V. Le, "Efficientdet: Scalable and efficient object detection," in *Proceedings of the IEEE/CVF Conference on Computer Vision and Pattern Recognition (CVPR)*, 2020, pp. 10 781–10 790.
- [43] N. Carion, F. Massa, G. Synnaeve, N. Usunier, A. Kirillov, and S. Zagoruyko, "End-to-end object detection with transformers," in *European conference on computer vision*. Springer, 2020, pp. 213–229.
- [44] M. Tan and Q. Le, "Efficientnet: Rethinking model scaling for convolutional neural networks," in *International Conference on Machine Learning (ICML)*. PMLR, 2019, pp. 6105–6114.
- [45] C.-Y. Wang, H.-Y. M. Liao, Y.-H. Wu, P.-Y. Chen, J.-W. Hsieh, and I.-H. Yeh, "Cspnet: A new backbone that can enhance learning capability of cnn," in *Proceedings of the IEEE/CVF conference on computer vision and pattern recognition workshops*, 2020, pp. 390–391.
- [46] G. Jocher, "mosaic augmentation," <https://github.com/ultralytics/yolov3>, (accessed 13 April 2022).
- [47] R. Chauhan, H. Kaur, and V. Chang, "Advancement and applicability of classifiers for variant exponential model to optimize the accuracy for deep learning," *Journal of Ambient Intelligence and Humanized Computing*, pp. 1–10, 2017.
- [48] A. Saleh, R. Sukaik, and S. S. Abu-Naser, "Brain tumor classification using deep learning," in *2020 International Conference on Assistive and Rehabilitation Technologies (iCareTech)*. IEEE, 2020, pp. 131–136.
- [49] M. I. Sharif, M. A. Khan, M. Alhussain, K. Aurangzeb, and M. Raza, "A decision support system for multimodal brain tumor classification using deep learning," *Complex & Intelligent Systems*, pp. 1–14, 2021.
- [50] H. Mohsen, E.-S. A. El-Dahshan, E.-S. M. El-Horbaty, and A.-B. M. Salem, "Classification using deep learning neural networks for brain tumors," *Future Computing and Informatics Journal*, vol. 3, no. 1, pp. 68–71, 2018.
- [51] M. A. Khan, I. Ashraf, M. Alhaisoni, R. Damas'evic'ius, R. Scherer, A. Rehman, and S. A. C. Bukhari, "Multimodal brain tumor classification using deep learning and robust feature selection: A machine learning application for radiologists," *Diagnostics*, vol. 10, no. 8, p. 565, 2020.
- [52] M. Aamir, Z. Rahman, Z. A. Dayo, W. A. Abro, M. I. Uddin, I. Khan, A. S. Imran, Z. Ali, M. Ishfaq, Y. Guan *et al.*, "A deep learning approach for brain tumor classification using mri images," *Computers and Electrical Engineering*, vol. 101, p. 108105, 2022.
- [53] J. S. Paul, A. J. Plassard, B. A. Landman, and D. Fabbri, "Deep learning for brain tumor classification," in *Medical Imaging 2017: Biomedical Applications in Molecular, Structural, and Functional Imaging*, vol. 10137. SPIE, 2017, pp. 253–268.
- [54] S. Deepak and P. Ameer, "Brain tumor classification using deep cnn features via transfer learning," *Computers in biology and medicine*, vol. 111, p. 103345, 2019.
- [55] H. Chegraoui, C. Philippe, V. Dangouloff-Ros, A. Grigis, R. Calmon, N. Boddaert, F. Frouin, J. Grill, and V. Frouin, "Object detection improves tumour segmentation in mr images of rare brain tumours," *Cancers*, vol. 13, no. 23, p. 6113, 2021.
- [56] S. R. Telrandhe, A. Pimpalkar, and A. Kendhe, "Brain tumor detection using object labeling algorithm & svm," *International Engineering Journal For Research & Development*, vol. 2, pp. 2–8, 2015.
- [57] N. Arunkumar, M. A. Mohammed, M. K. Abd Ghani, D. A. Ibrahim, E. Abdulhay, G. Ramirez-Gonzalez, and V. H. C. de Albuquerque, "K-means clustering and neural network for object detecting and identifying abnormality of brain tumor," *Soft Computing*, vol. 23, pp. 9083–9096, 2019.
- [58] A. Aleid, K. Alhussaini, R. Alanazi, M. Altwaimi, O. Altwijri, and A. S. Saad, "Artificial intelligence approach for early detection of brain tumors using mri images," *Applied Sciences*, vol. 13, no. 6, p. 3808, 2023.
- [59] M. Kang, C.-M. Ting, F. F. Ting, and R. C.-W. Phan, "Rcs-yolo: A fast and high-accuracy object detector for brain tumor detection," in *International Conference on Medical Image Computing and Computer-Assisted Intervention*. Springer, 2023, pp. 600–610.
- [60] F. Mercaldo, L. Brunese, F. Martinelli, A. Santone, and M. Cesarelli, "Object detection for brain cancer detection and localization," *Applied Sciences*, vol. 13, no. 16, p. 9158, 2023.
- [61] N. M. Dipu, S. A. Shohan, and K. A. Salam, "Brain tumor detection using various deep learning algorithms," in *2021 International Conference on Science & Contemporary Technologies (ICSCT)*. IEEE, 2021, pp. 1–6.
- [62] D. Suresha, N. Jagadisha, H. Shrisha, and K. Kaushik, "Detection of brain tumor using image processing," in *2020 Fourth International Conference on Computing Methodologies and Communication (ICCMC)*. IEEE, 2020, pp. 844–848.
- [63] K. Salc'in *et al.*, "Detection and classification of brain tumours from mri images using faster r-cnn," *Tehnic'ki glasnik*, vol. 13, no. 4, pp. 337–342, 2019.
- [64] Y. Bhanothu, A. Kamalakannan, and G. Rajamanickam, "Detection and classification of brain tumor in mri images using deep convolutional network," in *2020 6th international conference on advanced computing and communication systems (ICACCS)*. IEEE, 2020, pp. 248–252.
- [65] kaggle, "brain tumor dataset," <https://www.kaggle.com/>, (accessed: 15.01.2023).
- [66] roboflow, <https://blog.roboflow.com/advanced-augmentations/>, (accessed: 15.01.2023).
- [67] S. Ioffe and C. Szegedy, "Batch normalization: Accelerating deep network training by reducing internal covariate shift," in *International conference on machine learning*. pmlr, 2015, pp. 448–456.
- [68] S. Elfving, E. Uchibe, and K. Doya, "Sigmoid-weighted linear units for neural network function approximation in reinforcement learning," *Neural networks*, vol. 107, pp. 3–11, 2018.
- [69] A. F. Agarap, "Deep learning using rectified linear units (relu)," *arXiv preprint arXiv:1803.08375*, 2018.
- [70] K. He, X. Zhang, S. Ren, and J. Sun, "Spatial pyramid pooling in deep convolutional networks for visual recognition," *IEEE transactions on pattern analysis and machine intelligence*, vol. 37, no. 9, pp. 1904–1916, 2015.
- [71] T.-Y. Lin, P. Dolla' r, R. Girshick, K. He, B. Hariharan, and S. Belongie, "Feature pyramid networks for object detection," in *Proceedings of the IEEE conference on computer vision and pattern recognition*, 2017, pp. 2117–2125.
- [72] S. Liu, L. Qi, H. Qin, J. Shi, and J. Jia, "Path aggregation network for instance segmentation," in *Proceedings of the IEEE conference on computer vision and pattern recognition*, 2018, pp. 8759–8768.
- [73] A. Neubeck and L. Van Gool, "Efficient non-maximum suppression," in *18th international conference on pattern recognition (ICPR'06)*, vol. 3. IEEE, 2006, pp. 850–855.
- [74] M. Everingham, S. A. Eslami, L. Van Gool, C. K. Williams, J. Winn, and A. Zisserman, "The pascal visual object classes challenge: A retrospective," *International journal of computer vision*, vol. 111, pp. 98–136, 2015.